

See discussions, stats, and author profiles for this publication at: <https://www.researchgate.net/publication/244426398>

A Combined Quantum Chemistry and RRKM Calculation Predicts the $O(1D) + C_2H_6$ Reaction Can Produce Water Molecule in a Collision-Free Crossed Molecular Beam Environment

ARTICLE in THE JOURNAL OF PHYSICAL CHEMISTRY A · SEPTEMBER 2003

Impact Factor: 2.69 · DOI: 10.1021/jp027439t

CITATIONS

6

READS

12

6 AUTHORS, INCLUDING:



Ying-Chieh Sun

National Taiwan Normal University

32 PUBLICATIONS 373 CITATIONS

SEE PROFILE



Thanh Lam Nguyen

University of Texas at Austin

72 PUBLICATIONS 1,380 CITATIONS

SEE PROFILE



Hsiu-Feng Lu

Academia Sinica

23 PUBLICATIONS 330 CITATIONS

SEE PROFILE



Xueming Yang

Dalian Institute of Chemical Physics

176 PUBLICATIONS 2,980 CITATIONS

SEE PROFILE

Experimental and theoretical investigations of the O(1D) reaction with cyclopropane

Chia C. Wang, Jinian Shu, Jim J. Lin, Yuan T. Lee, Xueming Yang et al.

Citation: *J. Chem. Phys.* **116**, 8292 (2002); doi: 10.1063/1.1466468

View online: <http://dx.doi.org/10.1063/1.1466468>

View Table of Contents: <http://jcp.aip.org/resource/1/JCPSA6/v116/i19>

Published by the [American Institute of Physics](#).

Additional information on J. Chem. Phys.


Journal Homepage: <http://jcp.aip.org/>

Journal Information: http://jcp.aip.org/about/about_the_journal

Top downloads: http://jcp.aip.org/features/most_downloaded

Information for Authors: <http://jcp.aip.org/authors>

ADVERTISEMENT



AIPAdvances

Special Topic Section:
PHYSICS OF CANCER

Why cancer? Why physics? [View Articles Now](#)

Experimental and theoretical investigations of the $O(^1D)$ reaction with cyclopropane

Chia C. Wang

Department of Chemistry, National Taiwan University, Taipei, Taiwan

Jinian Shu and Jim J. Lin

Institute of Atomic and Molecular Science, Academia Sinica, Taipei, Taiwan

Yuan T. Lee

*Department of Chemistry, National Taiwan University, Taipei, Taiwan,
and Institute of Atomic and Molecular Science, Academia Sinica, Taipei, Taiwan*

Xueming Yang^{a)}

*Institute of Atomic and Molecular Science, Academia Sinica, Taipei, Taiwan,
Department of Chemistry, National Tsing Hua University, Hsinchu, Taiwan,
and Dalian Institute of Chemical Physics, Chinese Academy of Sciences, Dalian, China*

Thanh Lam Nguyen and Alexander M. Mebel

Institute of Atomic and Molecular Science, Academia Sinica, Taipei, Taiwan

(Received 20 August 2001; accepted 8 February 2002)

In this report, the $O(^1D) + c\text{-C}_3\text{H}_6$ reaction has been investigated using the universal crossed molecular beam technique. Angular resolved time-of-flight spectra have been measured for the observed reaction products in a single set of experiments. Four reaction channels have been observed clearly for this reaction. In addition to the $\text{OH} + \text{C}_3\text{H}_5$ channel, the two microchannels for C_2H_4 formation and the H-atom formation channel are also present. Different product angular distributions were measured for the observed product channels, indicating that each reaction channel occurs with distinctive dynamics. Branching ratios for all observed reaction channels have also been estimated. High-level theoretical calculations have been performed on the energetics of this reaction, indicating two major insertion pathways are likely responsible for most of the reaction channels.

© 2002 American Institute of Physics. [DOI: 10.1063/1.1466468]

I. INTRODUCTION

The O atom reactions with hydrocarbon molecules are important research topics in both combustion processes and atmospheric chemistry. The reactions of $O(^1D)$ with small alkane molecules, such as methane, ethane, propane, etc., have been investigated extensively during the last few decades.^{1–20} In the reactions with small alkanes, the insertion of the $O(^1D)$ atom into a (C–H) bond is the most important pathway for these reactions. These studies provide a rather complete picture of the $O(^1D)$ reaction dynamics with normal alkanes. However, the reaction dynamics of the $O(^1D)$ reaction with cyclic alkanes have not been studied previously. Since the electronic structures of cyclic alkanes are significantly different from normal alkanes, it would be interesting to know how the dynamics of the $O(^1D)$ reaction with cyclic alkanes is different from that with normal alkanes.

The reaction of $O(^1D)$ with cyclopropane has been studied in this work both experimentally and theoretically. Experimentally, the title reaction was studied using the crossed molecular beam method. Through both careful measurements and detailed analyses of the time-of-flight (TOF) spec-

tra and angular distribution of products from the crossed molecular beam study of the $O(^1D) + c\text{-C}_3\text{H}_6$ reaction, a rather complete dynamical picture of this reaction is constructed. A rather complete map of the energetics of all reaction pathways has been derived theoretically using *ab initio* calculations. Such a theoretical picture should be quite helpful for the interpretation of the experimental dynamical results.

The rest of this paper is divided into the following sections: Theoretical Reaction Energetics, Experiment, Results and Discussions, and Conclusions.

II. REACTION ENERGETICS AND PATHWAYS

Possible reaction pathways and energetics of the $O(^1D)$ reaction cyclopropane have been investigated using *ab initio* theoretical methods. The geometries of the reactants, products, various intermediates, and transition states for the $O(^1D) + c\text{-C}_3\text{H}_6$ reaction were optimized using the B3LYP (Ref. 21) method, in conjunction with the 6-311G(*d,p*) basis set. Vibrational frequencies, calculated at the B3LYP/6-311G(*d,p*) level, were used for characterization of stationary points, zero-point energy (ZPE) correction. All the stationary points were positively identified for minimum (number of imaginary frequencies NIMAG=0) or transition state (NIMAG=1). To obtain more accurate energies on the potential energy surface (PES), we employed the CCSD(T)

^{a)} Author to whom correspondence should be addressed. Electronic mail: xmyang@po.iam.s.sinica.edu.tw

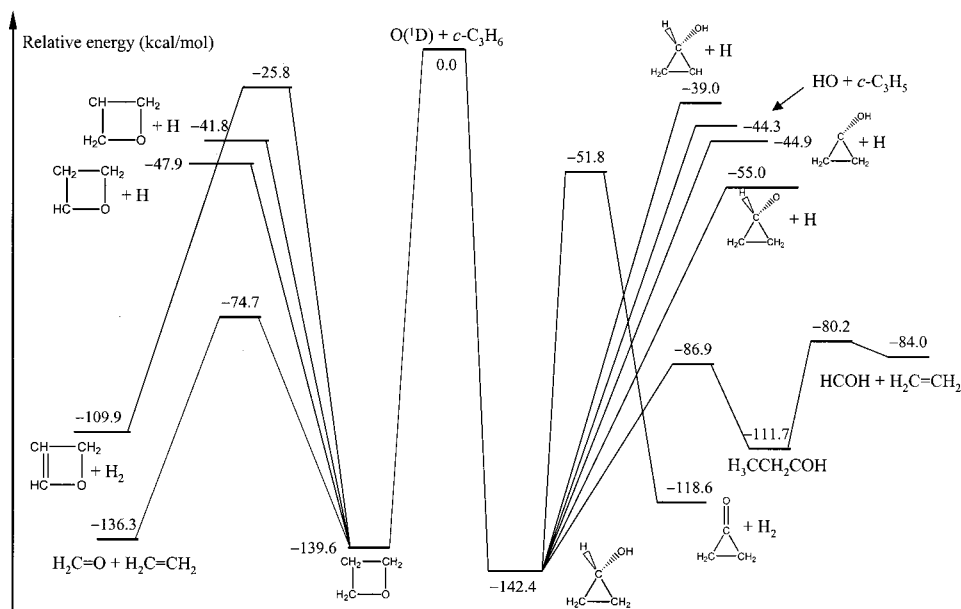


FIG. 1. Energy diagram for possible reaction channels of the bimolecular reaction of $O(^1D) + c\text{-C}_3\text{H}_6$ as calculated at the CCSD(T)/6-311+G(3df,2p)//B3LYP/6-311G(d,p) + ZPE [B3LYP/6-311(d,p)] level.

(Ref. 22) method with the large 6-311+G(3df,2p) basis set. The CCSD(T)/6-311+G(3df,2p)//B3LYP/6-311G(d,p)+ZPE[B3LYP/6-311G(d,p)] calculational scheme²³ has been shown to provide accuracies of 1–2 kcal/mol (Refs. 24–28) for atomization energies of the G2 test set of molecules. A similar CCSD(T)/B3LYP approach has been also demonstrated to be accurate for transition state energies.²⁹ The MOLPRO 2000 (Ref. 30) and GAUSSIAN 98 (Ref. 31) programs were employed for the PES calculations. The calculated energetics of related reaction pathways are shown in Fig. 1.

According to the *ab initio* calculations for the $O(^1D) + c\text{-C}_3\text{H}_6$ reaction involving vibrationally excited oxetane and cyclopropanol, the $\text{C}_2\text{H}_4 + \text{CH}_2\text{O}$ channel should be the main reaction products. These results are in good agreement with that obtained in the current crossed beam experiment. Analyses of all possible channels in detail including RRKM calculations will be reported in a future full paper.³²

III. EXPERIMENT

The apparatus used in this work is a newly built crossed molecular beam machine which has been described in detail elsewhere.³³ Briefly, the O atomic beam, generated using the photodissociation of O_2 at 157.6 nm in a skimmed O_2 pulsed beam, was crossed with a skimmed C_3H_6 beam at a fixed angle of 90° . The $^{18}\text{O}_2$ beam was used here instead of the normal O_2 beam in order to avoid the higher background at mass 17 in the detector. The $^{18}\text{O}_2$ beam was obtained by expanding a neat $^{18}\text{O}_2$ sample through a commercial pulsed valve with a risetime of about $50\mu\text{s}$, at a stagnation pressure of about 5 atm. The molecular beam was then skimmed by a sharp-edged skimmer with 2 mm diam orifice. The $^{18}\text{O}_2$ beam was then intercepted by an unpolarized 157.6 nm laser beam, generated by a Lambda Physik LPX210I F_2 laser, with a pulse energy of about 30 mJ at a repetition rate of 50 Hz. The $^{18}\text{O}(^1D)$ atomic beam generated from the 157 nm pho-

tolysis was skimmed once before entering the main chamber. $\text{O}(^3P)$ is also present in the O atom beam with the same amount to $\text{O}(^1D)$. In order to reduce the detector background from the beam, the $^{18}\text{O}_2$ beam was pointing in a direction that is about 60° off the detector axis plane such that the oxygen beam does not get into the detector easily (see Fig. 2 for the detailed experimental scheme used in this work). The F_2 laser beam was focused on a spot of $4\text{ mm(w)} \times 4\text{ mm(h)}$ in the interaction region by a spherical-cylindrical MgF_2 lens. Using the above focusing condition and laser power, the $^{18}\text{O}_2$ transition (cross section $\sigma = 6.8 \times 10^{-18}\text{ cm}^2$) at 157.6 nm can be easily saturated. The $c\text{-C}_3\text{H}_6$ beam was obtained by expanding a neat $c\text{-C}_3\text{H}_6$ sample at a stagnation pressure of about 5 atm through a carefully adjusted pulsed valve with a risetime of about $60\mu\text{s}$ and then skimmed once by a 1.5 mm orifice before enter-

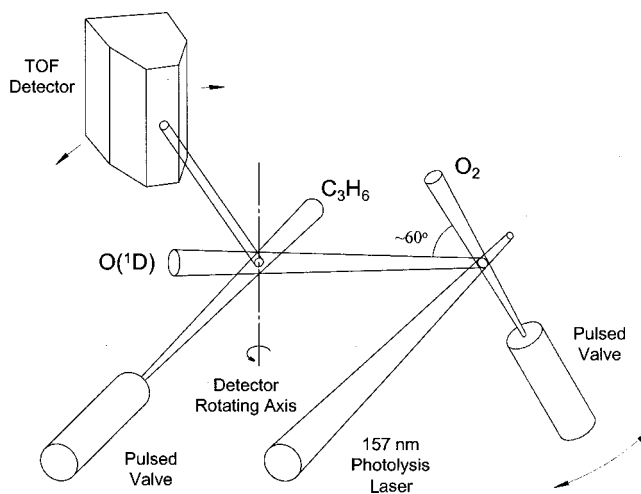


FIG. 2. The experimental configuration used in this study.

ing the main chamber. The ^{18}O atomic beam extracted from the $^{18}\text{O}_2$ photodissociation, the $c\text{-C}_3\text{H}_6$ molecular beam, and the rotating detector axis are all on the same plane. The velocity spread of the ^{18}O atomic beam is less than 2% according to our measurement. The collisional energy of the title reaction is about 9 kcal/mol in this experiment. The angular divergence of the ^{18}O atomic beam was about $\pm 3^\circ$. The speed of the $c\text{-C}_3\text{H}_6$ beam was about 840 m/s, with a speed ratio of about 9 and an angular divergence of about $\pm 2^\circ$. Reaction products scattered from the interaction region are detected by a mass-selective electron impact ionization detector with a time-of-flight resolution of about 4%.

The whole experiment was pulsed, and time zero was defined as the time when the beams were crossed. After flying about 25 cm from the crossed region, the neutral reaction products were ionized by a Brink's-type electron impact ionizer with electron energy of about 60 eV. The product ions were mass filtered by a quadrupole mass filter with a mass resolution larger than 200, and counted by a Daly ion detector. All time-of-flight (TOF) spectra shown here are measured with a time bin of 3 μs . The total product angular distributions were measured by rotating the detector. During the experiments described above, the vacuum in the detector ionization region was maintained at about 1×10^{-12} Torr or below.

The time-of-flight spectra and angular distributions of the neutral products measured in the laboratory (LAB) frame were simulated in order to obtain the product kinetic energy distribution (PKED) and product angular distribution (PAD) in the center-of-mass (CM) frame using a computer program. Basically, the simulations to the TOF spectra and the product laboratory angular distribution were carried out by using an iterative forward convolution program, starting with an initially guessed CM kinetic energy distributions and angular distribution. By comparing the calculated TOF spectra and the experimental TOF spectra, the initially guessed PKED is adjusted iteratively so that satisfactory fits to the TOF spectra are obtained. In the same simulation, the initially guessed CM PAD is also iteratively adjusted so that good agreement between the experimental and simulated PADs is reached. In a typical reaction, PKED is angular-dependent, therefore several CM kinetic energy distributions are necessary to describe the angular dependent kinetic energy distributions using linear interpolation in the simulation. The method to find out the minimum number of CM kinetic-energy-distributions required is usually by trial and error. In this way, the CM kinetic energy distributions and the CM angular distribution can be obtained. Simulation of TOF signals at a single mass with contributions from multiple reaction channels is done in a similar way by simply adding the contributions of a few different channels together. The relative ratios of different reaction channels contributing to the TOF signal at a specific mass could be determined interactively. The effects of the velocity spread (Δv) and the angular divergence of the two molecular beams are incorporated in the simulation.

IV. RESULTS AND DISCUSSIONS

Even though quite a few reaction channels are energetically accessible, only several of them were observed in this

work. In this experiment, signals at $m/e = 19, 31, 57$ were detected from the $\text{O}(^1D) + c\text{-C}_3\text{H}_6$ reaction. TOF spectra at different laboratory angles and the total product angular distribution were measured for all the above products. From detailed analyses of these data, several reaction channels have been identified. Systematic analyses on these data were carried out, and a reasonable dynamical picture is obtained. In the following paragraphs, the detailed analyses and results are described.

A. The $\text{H} + \text{C}_3\text{H}_5\text{O}$ channel

TOF signals were detected at mass 57 from the $^{18}\text{O}(^1D) + c\text{-C}_3\text{H}_6$ reaction and no product at higher masses than mass 57 from this reaction was observed. Since the reaction complex should be mass 60, the signals at mass 57 have to come from H atom or H_2 related reaction channels. If the mass 57 signal is from a neutral product at mass 57, then the mass 57 signal should come from the following two types of triple product channels: $\text{C}_3\text{H}_5\text{O} + \text{H} + \text{H}_2$ and $\text{C}_3\text{H}_5\text{O} + 3\text{H}$. However, these two types of channels are energetically not accessible. So the only two energetically accessible types of product channels that could be responsible for the mass 57 signals are the $\text{H}(\text{C}_3\text{H}_5\text{O})$ and $\text{H}_2(\text{C}_3\text{H}_4\text{O})$ formation channels. From the scattering angle range, and the kinetic energy release obtained from trial simulations, the main signal observed at mass 57 is more likely from H-atom product channels since the possible H_2 -product channels have significantly larger energy releases (see Fig. 1). The experimental TOF spectra of mass 57 at 8 different angles were measured carefully, and are shown in Fig. 3. In order to obtain the product kinetic energy distributions and the angular distribution in the CM frame, the TOF spectra and the angular distribution in the laboratory frame were simulated using the method described above. In the simulation, we assume that all signals are due to H-atom product formation. In simulations, the kinetic energy distribution for this channel is found to be angular dependent, indicating that reaction products scattering into different CM angles have somewhat different kinetic energy distributions. Therefore three different CM kinetic energy distributions at 0° , 40° , and 180° were used in the simulation. The obtained PKEDs are shown in Fig. 4, while the product CM angular distribution (summed products at each angle over different kinetic energies) used in the simulation is shown in Fig. 5. The simulated TOF spectra also shown in Fig. 3 are generally in good agreement with the experimental TOF spectra, and the experimental and the simulated product angular distributions are also in good agreement with each other. From the experimental results described above, the $\text{C}_3\text{H}_5\text{O}$ radical products are only slightly backward scattered with respect to the O atom beam, indicating that the observed reaction products are mainly produced via a long-lived complex, which is likely formed through an insertion channel. The small amount of extra slightly backward scattering products could come from some direct reaction process or shorter-lived complex. The high kinetic energy cutoff (~ 55 kcal/mol) of the PKEDs seems to be quite close to the theoretical energetic limit of the H-atom elimination from the OH group in the "hot" cyclopropanol complex (see Fig. 1), indicating that the O atom insertion

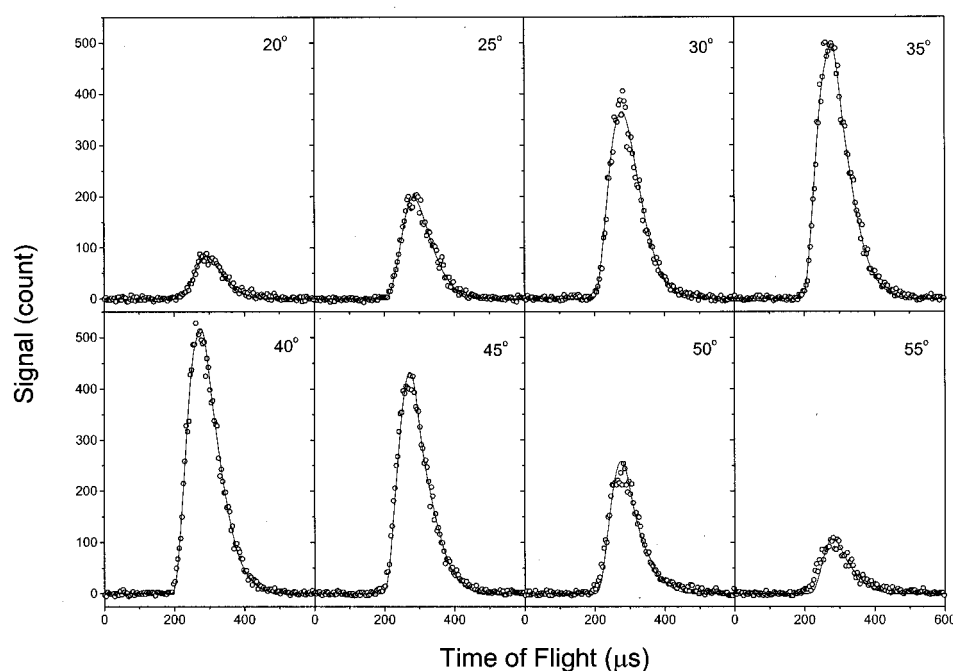


FIG. 3. TOF spectra at $m/e=57$ at eight different laboratory angles. The open circles represent the experimental data, while the solid lines are the simulated results.

into one of the six C–H bonds is an important mechanism for the observed H-form formation products. However, we could not totally rule out other possible contributing channels indicated in Fig. 1, in which the energetic limits of these channels are lower than the H-atom formation from the “hot” cyclopropanol complex pathway. One of the H-atom formation channels is the “hot” oxetane complex, which is likely formed via the O-atom barrierless insertion into a C–C bond in cyclopropane. This mechanism is actually quite interesting since an oxygen bridged ring compound is formed in this process.

Even though the agreement between experimental and simulated TOF spectra is quite good generally, there is still some disagreement at the front edge of the TOF spectra at some LAB angles. It seems that there is some small extra faster contribution in the TOF spectra. Since the H-atom should not be any faster because of the energetic limit (~ 55

kcal/mol) for the H-atom channels, the small extra contribution is likely from the H_2 formation channels, which have much larger available energies for the two possible channels (see Fig. 1). The contribution of the H_2 formation channels is, however, quite small and overlapped with the radical product signals from the H-atom formation channels. Therefore, it is difficult to separate the possible H_2 signals from the large H-atom channel signals quantitatively, and any quantitative treatment bears no significant physical meanings.

B. The $C_2H_4 + CH_2O/CHOH$ channel

Signals at mass 31 were also detected from the $^{18}O(^1D) + c-C_3H_6$ reaction. TOF spectra at mass 31 ($HC^{18}O^+$) were measured at 11 LAB angles. Nine of these TOF spectra are shown in Fig. 6. The measured product

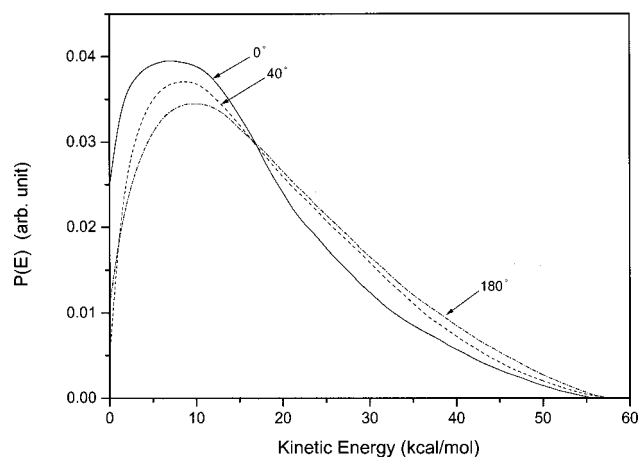


FIG. 4. The CM product kinetic energy distributions obtained from simulating the TOF spectra shown in Fig. 3. Three distributions at three CM angles are used in the simulation.

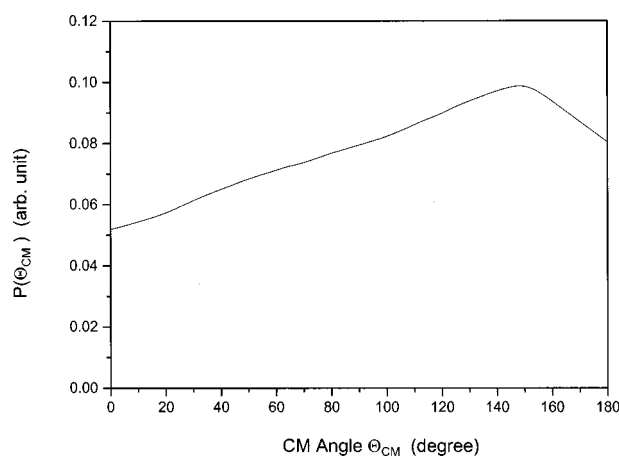


FIG. 5. The CM angular distribution of the H atom and H_2 formation channels obtained from simulating the TOF spectra at mass 57.

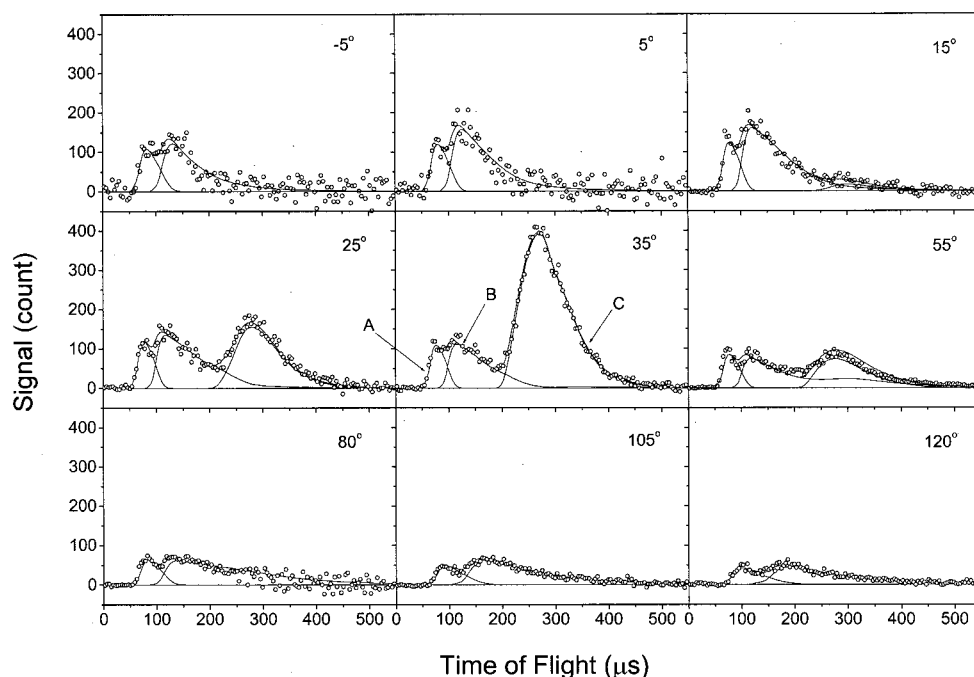


FIG. 6. TOF spectra at $m/e=31$ at eleven different laboratory angles. The open circles represent the experimental data, while the solid lines are the simulated results. There are three different contributions used in the simulations.

laboratory angular distribution for these TOF signals is shown in Fig. 7. From the TOF spectra, there are apparently three distinctive peaks, indicating three different channels are contributing to the signal at mass 31. The slowest peak (peak C) in the TOF spectra is very similar to the TOF features in Fig. 3, and they could all be simulated as the dissociative ionization signal of the radical products ($C_3H_5^{18}O$) from the H atom formation channels. Therefore, this peak is clearly due to the radical products from the H formation channels. The two peaks (peak A and peak B) in the front should come from reaction channels with comparable product masses and kinetic energy depositions. Therefore, these fast products are unlikely from H and H_2 formation channels. Because the HCO^+ ion is very stable, it is likely produced from dissociative ionization of some unstable parent products. Since no product has been detected in the mass range between mass

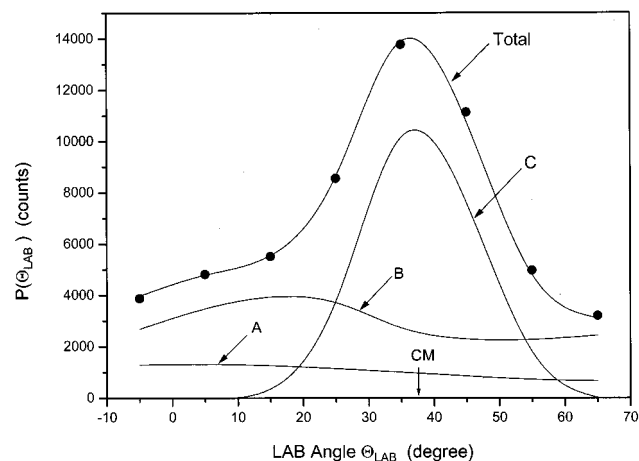


FIG. 7. Laboratory angular distribution of products at $m/e=31$. The black circles are the experimental data, while the solid line is the simulated results. There are three different contributions used in the simulations.

31 and mass 56, the faster HCO^+ ions are quite possibly coming from either $HC^{18}OH$ and/or $H_2C^{18}O$ products. There are two possible reaction channels to produce these two species: $HCOH + C_2H_4$ and $H_2CO + C_2H_4$. These two channels also have exactly the same product mass ratio, 32 ($HCOH$ or H_2CO): 28 (C_2H_4). From the energetic diagram, these two channels are both energetically accessible. Therefore, we believe that the two observed faster features (peak A and peak B) are due to the $H_2CO/HCOH + C_2H_4$ channels. We have tried to simulate the two faster features (peak A and peak B) together using a single PKED and a single CM angular distribution; the results are less than satisfactory. This is mainly due to the fact that the two fast features (peak A and peak B) appear to have somewhat different scattering angular distributions. Therefore, two distinctive contributions with different CM kinetic energy distributions and angular distributions were used to simulate the two features in the TOF spectra. The results are shown in Fig. 8 and Fig. 9, respectively. Since the two features (peak A and peak B) are overlapped, there are clearly some serious correlations between the two contributions in the overlapped region. From the above analyses, it is clear that the two new features have somewhat different angular distributions, implying different dynamical natures of the two observed features. The faster feature (curve A in Fig. 8) shows a rather forward-backward symmetric angular distribution, while the slower feature (curve B in Fig. 8) shows a somewhat backward angular distribution.

From the above results, two dynamical pathways are present in the likely C_2H_4 formation process. The nature of these two features is a more interesting issue. According to the above analysis, the two features (peaks A and B) are likely to come from the following two channels: $HCOH + C_2H_4$ and $H_2CO + C_2H_4$. From the energetic diagram, the available energy for the $H_2CO + C_2H_4$ channel is about 136 kcal/mol, while that for the $HCOH + C_2H_4$ channel is about

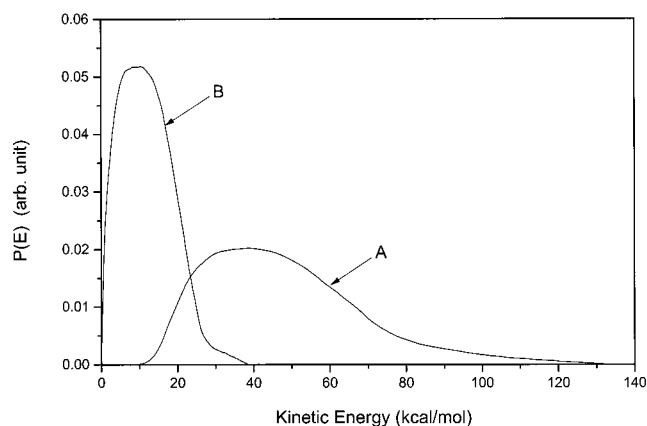


FIG. 8. The two CM product kinetic energy distributions obtained from simulating the two faster features in the TOF spectra (mass 31) shown in Fig. 6.

84 kcal/mol. From the CM kinetic energy distributions shown in Fig. 9, the energetic limit of the faster component (A) of the two contributions (A and B) is about 130 kcal/mol, which agrees quite well with the available energy of the $H_2CO + C_2H_4$ channel. Therefore, it is reasonable to assign the faster contribution (A) to the $H_2CO + C_2H_4$ channel. The nature of the slower contribution (B) observed at mass 31 is, however, more ambiguous. Obviously the slower contribution (B) is dynamically quite different from the faster contribution (A) because of its distinctive angular distribution. From the simulation, the energetic limit of the slower contribution is about 40 kcal/mol. However, there is a rather significant uncertainty in this limit due to the correlations in simulating the two features. Nevertheless, this limit appears to be significantly lower than the available energy of the $HCOH + C_2H_4$ channel, which is about 84 kcal/mol. Therefore it is somewhat questionable to assign this slower feature to the $HCOH + C_2H_4$ channel. It is still possible, however, that this channel is from the $HCOH + C_2H_4$ channel since the mismatch between the energetic limit and the available energy could be due to the fact that available energy is mostly distributed into the internal degrees of freedom of the two

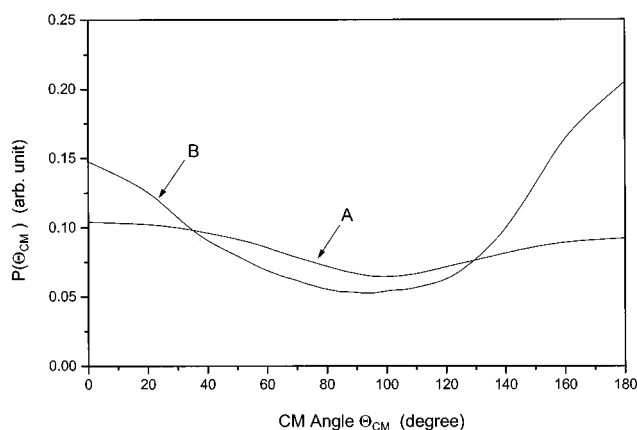


FIG. 9. The two CM product angular distributions obtained from simulating the faster two features in the TOF spectra at mass 31 (Fig. 6) and the laboratory angular distribution (Fig. 7).

molecular products. Furthermore, this feature could also come from other sources, such as electronically excited product channels of $H_2CO + C_2H_4$ or $HCOH + C_2H_4$. Notice that the adiabatic excitation energy for the first excited state of H_2CO is 80.7 kcal/mol,³⁴ which leaves 55.6 kcal/mol of available energy for the $H_2CO(S_1) + C_2H_4$ products.

The presence of the $H_2CO + C_2H_4$ channel is quite interesting. From the energetic diagram, this reaction channel should be a direct product from the “hot” oxetane complex formed through the $O(^1D)$ insertion into the C–C bond (see Fig. 1). Therefore, we believe that the observation of this channel is a clear experimental evidence of the $O(^1D)$ atom insertion into a C–C bond, which is normally difficult to occur. From our previous studies of the $O(^1D)$ reactions with small alkanes, $O(^1D)$ normally inserts into a C–H bond, which is somewhat less difficult because the H atom is lighter and easier to displace. It is reasonable to believe that the insertion of $O(^1D)$ into the C–C bond in cyclopropane is made easier due to the banana-type character of the C–C bond, in which the electronic cloud of the C–C bond is more accessible than for normal alkanes because of its banana shape. An interesting question regarding this process is whether the breaking up of the C–C and C–O bonds in the “hot” oxetane complex is simultaneous or stepwise that involves a ring-opening process. Our present calculations show that this reaction occurs in one step with simultaneous rupture of two bonds in the ring. A possible $HCOH + C_2H_4$ channel is also quite interesting since this channel is likely produced from the O atom insertion into the C–H bond. In order to form the $HCOH + C_2H_4$ channel, the “hot” cyclopropanol must go through a ring-opening process first. Relative importance of this pathway is also an interesting issue. Theoretical calculations of rate constants based on the *ab initio* results in this paper are desirable in order to clarify the relative importance of these channels.

C. The $OH + C_3H_5$ channel

^{18}OH products were detected at $m/e = 19$, indicating the existence of the $^{18}OH + C_3H_5$ channel. TOF spectra were measured at nine different lab angles, which are shown in Fig. 10. OH products are normally difficult to detect using conventional universal crossed beam apparatus because of the high background at mass 17 in the detector. In order to avoid such problems, $^{18}O_2$ beam was used to generate the $^{18}O(^1D)$ beam in this work instead of normal O_2 . As a result, the product ^{18}OH should be detected at mass 19 where the interference caused by the H_2O background in the detector is reduced significantly.

Reasonable fits to the TOF spectra of the ^{18}OH product at different lab angles have been obtained using a single product kinetic energy distribution (see Fig. 11). The ^{18}OH product CM angular distribution $P(\Theta_{CM})$ used in the fitting is shown in Fig. 12. From the results described above, it is obvious that the ^{18}OH products are slightly forward scattered with respect to the ^{18}O atom beam direction, implying that an insertion-type mechanism should be mainly responsible for this reaction channel, though there is some small possible contribution from a direct abstraction mechanism (pick-up at

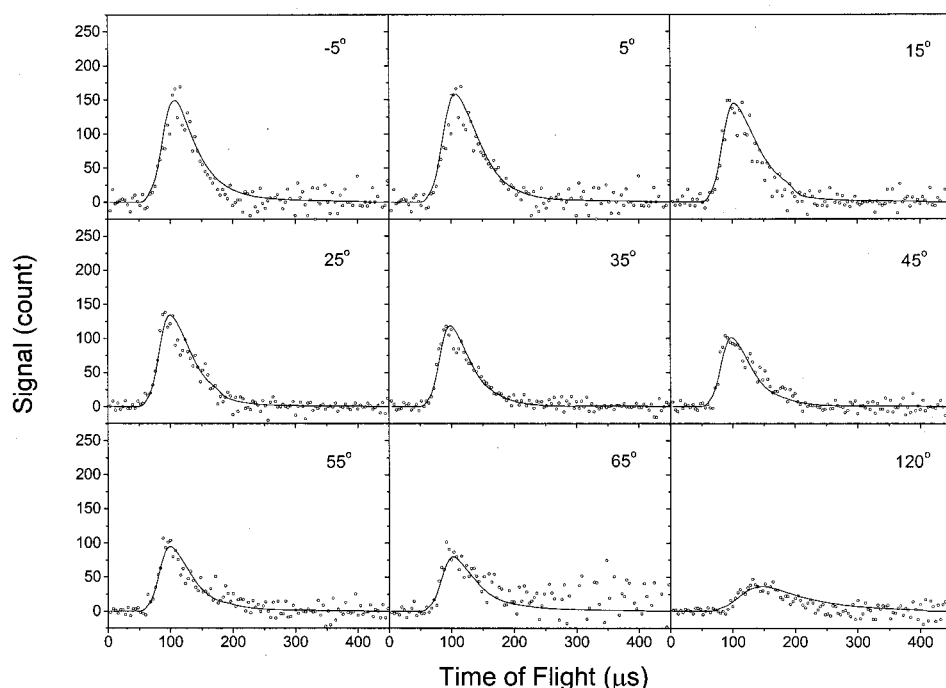


FIG. 10. TOF spectra at $m/e=19$ (OH) at nine different laboratory angles. The open circles represent the experimental data, while the solid lines are the simulated results.

larger impact parameters) that may be responsible for the forward scattered OH products. Since OH is formed in the reaction, the most likely reaction pathway should be the C–H bond insertion mechanism in which “hot” cyclopropanol complex is formed. This is also the most direct pathway to form the OH product. The energetic cutoff of the PKED for the OH channel is also consistent with the OH + $c\text{-C}_3\text{H}_5$ channel via the mechanism of O insertion into the C–H bond (see Fig. 1). Other possible mechanism such as O atom insertion into the C–C bond appears less likely since it requires significant structural rearrangement to form the OH product.

D. Relative branching ratios

The relative branching ratios for the reaction channels have been determined by measuring relative signals at differ-

ent masses that are detectable. Contributions from different channels to each cracked mass ion are obtained by simulating all TOF spectra for all observed masses. In the simulation, the detection efficiency is assumed to be the same for all detectable species. In addition, certain corrections, such as the reaction kinematics as well as the different detection efficiencies for products with different speeds using the electron impact ionizer, are made in the simulations. Based on this approximation, the relative branching of the two C_2H_4 formation channels is determined to be about 61%, while other channels count the rest 39%. Among the other channels, the OH formation channel was estimated to be 30%, while the H formation channel was about 9%. The molecular hydrogen formation channel seems present, but it should not be important ($<1\%$).

The relative branching ratio obtained for the four observed channels are listed in the following:

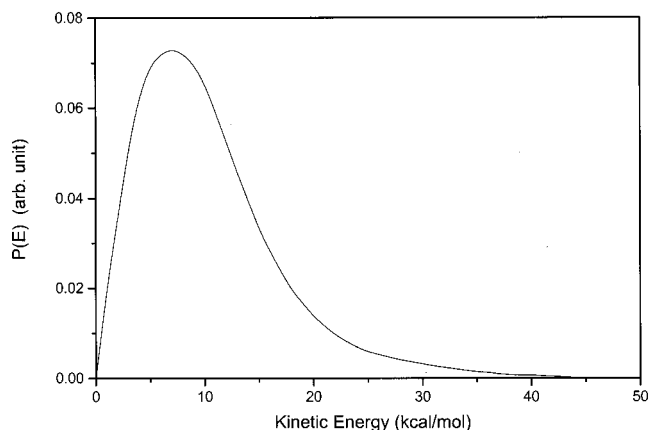


FIG. 11. The CM product kinetic energy distribution obtained from simulating the TOF spectra shown in Fig. 10.

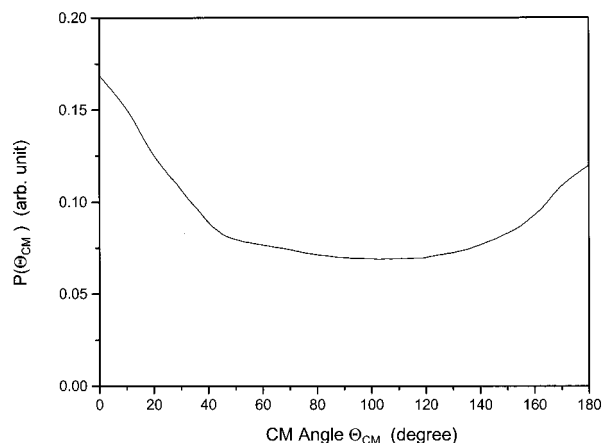
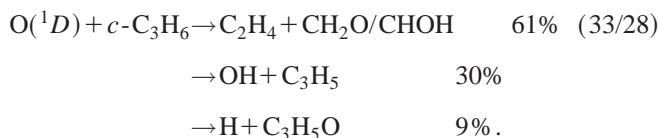


FIG. 12. The CM angular distribution of product observed at mass 19 obtained from simulating the TOF spectra (Fig. 10).



It should be noted that in addition to the O(¹D) atom in the O atom beam, there is also an equal amount of O(³P) in the beam. It is expected that O(¹D) should be more reactive than O(³P). No clear experimental evidence of the O(³P) reaction is detected. *Ab initio* calculations have also been performed on the O(³P) reaction with cyclopropane; no insertion pathway has been found for this reaction. The reaction barrier for the abstraction channel of the O(³P) reaction to form OH + *c*-C₃H₅ is calculated to be about 9.4 kcal/mol, indicating that this reaction should not be very significant in the present experimental study since the collisional energy at which this experiment was carried out is about 9 kcal/mol.

V. CONCLUSIONS

From the above investigations, four different channels have been clearly experimentally identified in the O(¹D) + *c*-C₃H₆ reaction using the crossed molecular beam method. Product kinetic energy distributions and angular distributions have been determined for all observed reaction channels. Each of these channels shows distinctive dynamical behaviors. Detailed experimental results indicate that the O(¹D) atom reaction likely proceeds via two main insertion mechanisms: O insertion into the C–H bond and O atom insertion into the C–C bond. This dynamical picture is supported by the theoretical calculations in this work. Theoretical calculations also indicate that the O(³P) reaction should not be important in this experiment. More theoretical studies on this reaction are desirable, however, in order to understand the dynamics of this complicated reaction more clearly.

ACKNOWLEDGMENTS

This work is supported by the Academia Sinica, the National Science Council of Taiwan, and partially by the China Petroleum Company.

¹C.-L. Lin and W. B. Demore, J. Phys. Chem. **77**, 863 (1972).

²W. Tsang, Int. J. Chem. Kinet. **8**, 193 (1976), and references therein.

³R. I. Greenberg and J. Heicklen, Int. J. Chem. Kinet. **4**, 417 (1972).

⁴P. Casavecchia, R. J. Buss, S. J. Sibener, and Y. T. Lee, J. Chem. Phys. **73**, 6351 (1990); **73**, 6352 (1990).

⁵S. Satyapal, J. Park, R. Bersohn, and B. Katz, J. Chem. Phys. **91**, 6873 (1989).

⁶A. C. Luntz, J. Chem. Phys. **73**, 1143 (1980).

⁷S. G. Cheskis, A. A. Iogansen, P. V. Kulakov, I. Y. Razuvaev, O. M. Sarkisov, and A. A. Titov, Chem. Phys. Lett. **155**, 37 (1989).

⁸Y. Matsumi, K. Tonokura, Y. Inagaki, and M. Kawasaki, J. Phys. Chem. **97**, 6816 (1993).

⁹C. R. Park and J. R. Wiesenfeld, J. Chem. Phys. **95**, 8166 (1991).

¹⁰M. Brouard, S. Duxon, P. A. Enriquez, and J. P. Simons, J. Chem. Soc., Faraday Trans. **89**, 1435 (1993); M. Brouard, S. P. Duxon, and J. P. Simons, Isr. J. Chem. **34**, 67 (1994).

¹¹R. D. van Zee and J. C. Stephenson, J. Chem. Phys. **102**, 6946 (1995).

¹²P. M. Aker, J. J. A. O'Brien, and J. J. Sloan, J. Chem. Phys. **84**, 745 (1986).

¹³Y. Rudich, Y. Hurwitz, G. J. Frost, V. Vaida, and R. Naaman, J. Chem. Phys. **99**, 4500 (1993).

¹⁴Y. Hurwitz, Y. Rudich, and R. Naaman, Chem. Phys. Lett. **215**, 674 (1993).

¹⁵R. D. van Zee, J. C. Stephenson, and M. P. Casassa, Chem. Phys. Lett. **223**, 167 (1994).

¹⁶T. Suzuki and E. Hirota, J. Chem. Phys. **98**, 2387 (1993).

¹⁷R. Schott, J. Schluter, and K. Kleineremanns, J. Chem. Phys. **102**, 8371 (1995).

¹⁸J. Schluter, R. Schott, and K. Kleineremanns, Chem. Phys. Lett. **213**, 262 (1993).

¹⁹W. Hack and H. Thiesemann, J. Phys. Chem. **99**, 17364 (1995).

²⁰R. A. Brownsword, M. Hillenkamp, P. Schmiechen, H.-R. Volpp, and H. P. Upadhyaya, J. Phys. Chem. **102**, 4438 (1998).

²¹A. D. Becke, J. Chem. Phys. **98**, 5648 (1993); **96**, 2155 (1992); **97**, 9173 (1992); C. Lee, W. Yang, and R. G. Parr, Phys. Rev. B **37**, 785 (1988).

²²G. D. Purvis and R. J. Bartlett, J. Chem. Phys. **76**, 1910 (1982); G. E. Scuseria, C. L. Janssen, and H. F. Schaefer III, *ibid.* **89**, 7382 (1988); G. E. Scuseria and H. F. Schaefer III, *ibid.* **90**, 3700 (1989); (d) J. A. Pople, M. Head-Gordon, and K. Raghavachari, *ibid.* **87**, 5968 (1987).

²³C. W. Bauschlicher, Jr. and H. Partridge, J. Chem. Phys. **103**, 1788 (1995); Chem. Phys. Lett. **240**, 533 (1995).

²⁴A. M. Mebel, K. Morokuma, and M. C. Lin, J. Chem. Phys. **103**, 7414 (1995).

²⁵C. W. Bauschlicher and H. Partridge, J. Chem. Phys. **103**, 1788 (1995).

²⁶L. A. Curtiss, K. Raghavachari, P. C. Redfern, and J. A. Pople, J. Chem. Phys. **106**, 1063 (1997).

²⁷L. A. Curtiss, K. Raghavachari, P. C. Redfern, and J. A. Pople, J. Chem. Phys. **109**, 42 (1998).

²⁸L. A. Curtiss, K. Raghavachari, P. C. Redfern, V. Rassolov, and J. A. Pople, J. Chem. Phys. **109**, 7764 (1998).

²⁹A. M. Mebel, K. Morokuma, and M. C. Lin, J. Chem. Phys. **103**, 7414 (1995); A. M. Mebel, K. Morokuma, M. C. Lin, and C. F. Melius, J. Phys. Chem. **99**, 1900 (1995); A. M. Mebel, K. Morokuma, and M. C. Lin, J. Chem. Phys. **103**, 3440 (1995).

³⁰MOLPRO is a package of *ab initio* programs written by H.-J. Werner and P. J. Knowles with contributions from J. Almlöf, R. D. Amos, M. J. O. Deegan, S. T. Elbert, C. Hampel, W. Meyer, K. Peterson, R. Pitzer, A. J. Stone, P. R. Taylor, and R. Lindh.

³¹M. J. Frisch, G. W. Trucks, H. B. Schlegel, *et al.* GAUSSIAN 98, Revision A.7 Gaussian, Inc., Pittsburgh, PA, 1998.

³²T. L. Nguyen *et al.* (unpublished).

³³J. J. Lin, D. W. Hwang, S. Harich, Y. T. Lee, and X. Yang, Rev. Sci. Instrum. **69**, 1642 (1998).

³⁴A. K. Shah and D. C. Moule, Spectrochim. Acta, Part A **34A**, 749 (1978); P. Jensen and P. R. Bunker, J. Mol. Spectrosc. **94**, 114 (1982).